AGU ADVANCING EARTH AND SPACE SCIENCES

Geophysical Research Letters

RESEARCH LETTER
10.1029/2023GL107121

Investigating Diurnal and Seasonal Cycles of Vegetation Optical Depth Retrieved From GNSS Signals in a Broadleaf Forest

Yitong Yao[1], Vincent Humphrey[2,3], Alexandra G. Konings[4], Yujie Wang[1], Yi Yin[5], Nataniel Holtzman[4], Jeffrey D. Wood[6], Yinon Bar-On[1], and Christian Frankenberg[1,7]

[1]Division of Geological and Planetary Sciences, California Institute of Technology, Pasadena, CA, USA, [2]Department of Geography, University of Zürich, Zürich, Switzerland, [3]Federal Office of Meteorology and Climatology MeteoSwiss, Zürich, Switzerland, [4]Department of Earth System Science, Stanford University, Stanford, CA, USA, [5]Department of Environmental Studies, New York University, New York, NY, USA, [6]School of Natural Resources, University of Missouri, Columbia, MO, USA, [7]Jet Propulsion Laboratory, California Institute of Technology, Pasadena, CA, USA

Key Points:

- Sub-hourly Vegetation Optical Depth (VOD) retrieved from Global Navigation Satellite Systems attenuation relates to soil and leaf water dynamics
- Daily maximum VOD correlates well with field measurements of predawn leaf water potential
- Plant transpiration can be reconstructed from VOD principal components

Supporting Information:

Supporting Information may be found in the online version of this article.

Correspondence to:

Y. Yao and C. Frankenberg,
yyao2@caltech.edu;
cfranken@caltech.edu

Citation:

Yao, Y., Humphrey, V., Konings, A. G., Wang, Y., Yin, Y., Holtzman, N., et al. (2024). Investigating diurnal and seasonal cycles of Vegetation Optical Depth retrieved from GNSS signals in a broadleaf forest. *Geophysical Research Letters*, *51*, e2023GL107121. https://doi.org/10.1029/2023GL107121

Received 1 NOV 2023
Accepted 1 MAR 2024

Abstract Vegetation Optical Depth (VOD) has emerged as a valuable metric to quantify water stress on vegetation's carbon uptake from a remote sensing perspective. However, existing spaceborne microwave remote sensing platforms face limitations in capturing the diurnal VOD variations and global products lack site-level validation against plant physiology. To address these challenges, we leveraged the Global Navigation Satellite System (GNSS) L-band microwave signal, measuring its attenuation by the canopy of a temperate broadleaf forest using a pair of GNSS receivers. This approach allowed us to collect continuous VOD observations at a sub-hourly scale. We found a significant seasonal-scale correlation between VOD and leaf water potential. The VOD diurnal amplitude is affected by soil moisture, plant transpiration and leaf surface water. Additionally, VOD can help independently estimate plant transpiration. Our findings pave the way for a deeper understanding of response of the vegetation to water stress at finer temporal scales.

Plain Language Summary Microwave satellite measurements offer valuable insights into Vegetation Optical Depth (VOD), which reflects the amount of water present in plants. However, most VOD products currently available only offer observations at two times of the day, which fail to capture the variations of VOD over the course of the day. In this study, we installed Global Navigation Satellite System (GNSS) signal receivers at the top and bottom of a temperate broadleaf forest canopy located at a flux tower in Missouri, USA. This setup allowed us to obtain continuous observations of VOD at sub-hourly scale. The strong correlation observed between GNSS VOD and local leaf water potential suggests that this robust and cost-effective technique can complement other labor-intensive measurements. The VOD diurnal amplitude is influenced by soil water content, evapotranspiration, and leaf surface water in the form of dew and interception. GNSS VOD also exhibits the potential to aid in estimating plant transpiration, which can be further used for partitioning evapotranspiration. The investigation of plant water content dynamics in this study will enhance our understanding of the carbon-water coupling at a finer temporal scale.

1. Introduction

Understanding the dynamics of water moving through the soil-plant-atmosphere continuum is of great importance, as it directly impacts essential physiological processes of photosynthesis and transpiration, ecosystem functioning, and climate regulation (Gentine et al., 2019; Harris et al., 2022; McDowell et al., 2022). The amount of water stored within plants can be a powerful empirical proxy of these processes. Traditionally, whole-plant water content has been measured using labor-intensive techniques such as dendrometers (Barraclough et al., 2020), or time domain reflectometry and frequency domain reflectometry instruments (He et al., 2021; Matheny et al., 2015). However, these in situ measurements face challenges in up-scaling to ecosystem scale and are limited in their temporal and spatial coverage (Novick et al., 2022).

Remote sensing plays a crucial role in studying plant water content and associated processes, providing observations at larger spatial scales. Microwave remote sensing is particularly valuable in this regard, as the water within vegetation attenuates the microwave signal and the extinction of the microwave radiation in the canopy is used to retrieve Vegetation Optical Depth (VOD). VOD contains information related to vegetation biomass (Fan

et al., 2019) and gravimetric water content, which can be related to water availability (Zhang et al., 2019), and various physiological indicators including leaf water potential (Jagdhuber et al., 2021) and overall plant health (Konings et al., 2019). Microwave satellite VOD products have also been used for monitoring vegetation dynamics (Anderegg et al., 2018; Bueso et al., 2023; Smith et al., 2022; Yang et al., 2022).

However, current VOD observations still have limitations. First, most microwave remote sensing products are obtained from sun-synchronous satellite platforms, which provide observations at only two specific local pass times in most latitudes. Consequently, the full diurnal variations in plant water content cannot be captured. For instance, Soil Moisture and Ocean Salinity and Soil Moisture Active Passive have local overpass times of 6 a.m./p.m. (Zhang et al., 2021). To overcome this limitation, Konings et al. (2021) suggested the use of geostationary satellites or a constellation of small satellites with different overpass times. By acquiring observations throughout the day, this approach could better constrain ecosystem dynamics, such as the vegetation response to water stress, as diurnal VOD variations primarily arise from variations in canopy water rather than biomass change. Additionally, given multiple processes contained in the satellite VOD measurements, disentangling their individual contribution remains challenging. Lastly, coarse-scale spaceborne VOD products lack ground-based references and direct connections with plant physiological indicators. Given that an individual pixel often covers diverse tree species and hydrological conditions, a dense observation network is required for validation. The challenges in achieving such a requirement hinder a comprehensive understanding of the complex mechanisms underlying plant water dynamics and their effect on carbon-water interactions. As measurements of other common physiological indicators related to plant water content, such as leaf water potential (Wood et al., 2023), are often labor-intensive, establishing links between ground-based measurements to proxies observable from space presents a promising strategy for complementing existing observations (Humphrey & Frankenberg, 2023). Such a linkage also serves as validation, facilitating the broader application of microwave-based VOD in data assimilation in terrestrial ecosystem models (Konings et al., 2019).

Here, we leverage recent advancements in measuring the attenuation effect of vegetation canopies on microwave signals from the Global Navigation Satellite Systems (GNSS) (Humphrey & Frankenberg, 2023; Rodriguez-Alvarez et al., 2011). We build on a data set from two GNSS signal receivers installed at the top and bottom of a vegetation canopy at the Ozark AmeriFlux (MOFLUX) site in Missouri, USA. Humphrey and Frankenberg (2023) showed that VOD can be retrieved from this GNSS receiver signal, resulting in continuous VOD observations. In this work, GNSS VOD spans from April 2021 to October 2022 at the sub-hourly time scale. This high-resolution ground-level GNSS VOD proves valuable for investigating the diurnal cycle of VOD and for disentangling the drivers of water content dynamics. The primary objective of this study is to use a high-frequency GNSS-based time series to interpret the diurnal and seasonal cycles of VOD. Specifically, we decomposed the GNSS VOD diurnal cycle and tested the relationship of VOD diurnal amplitude with various factors. Besides the GNSS VOD observation data, we also employed a land surface model (CliMA-Land) to compare with the main modes of variability observed in GNSS VOD. VOD reflects canopy water storage, which plays a crucial role in supplying water for plant transpiration. We show evidence that the changes in the diurnal amplitude of VOD can offer valuable insights into estimating the plant transpiration.

2. Materials and Methods

2.1. Field Data

2.1.1. General Site Information

The experiment was conducted at the MOFLUX site, situated in central Missouri, USA (38.7°N 92.2°W; AmeriFlux ID US-MOz). This location falls within the warm, humid and continental climate zones. The mean annual temperature is 13°C and the mean annual precipitation is 1,140 mm. The forest is of the oak-hickory type. Important tree species that are subject to routine measurements of predawn leaf water potential in the area are white oak, black oak, sugar maple, shagbark hickory, eastern redcedar and white ash (Wood et al., 2023). This drought-prone site experiences frequent late summer water stress, as observed from periodic leaf water potential measurements (Gu et al., 2015, 2016a).

Regular predawn leaf water potential ($\Psi_{pd,leaf}$) measurements started in 2004, and are conducted on a weekly to bi-weekly basis during the growing season to enable characterization of community water status (Gu, Pallardy,

Hosman, & Sun, 2016; Gu, Pallardy, Yang, et al., 2016). Leaf area index (LAI) measurements were also obtained at a weekly to bi-weekly interval (Wood et al., 2022).

For our study, we used half-hourly measurements of evapotranspiration (ET), air temperature, rainfall, relative humidity, vapor pressure deficit (VPD) and surface soil moisture content (SMC) at a depth of 5 cm. A complete description of the micrometeorological instrumentation and data processing is available in Gu, Pallardy, Yang, et al. (2016).

2.1.2. GNSS VOD

Two Septentrio PolaRx5e GNSS receivers equipped with PolaNt-x MF right-hand circular polarized (RHCP) GNSS antennas were deployed, allowing us to measure multi-constellation GNSS signals. One receiver was positioned above the forest canopy as an open-sky reference, while the other receiver was placed beneath the forest canopy to measure the attenuation by vegetation. From the signal-to-noise ratios (SNR) of both GNSS receivers we derived the canopy VOD following Humphrey and Frankenberg (2023), also accounting for the impact of angular heterogeneity on the signal intensity. Our observations spanned from April 2021 to October 2022. This period allowed us to investigate the seasonal and diurnal dynamics of vegetation water content within the study area.

2.2. Modeling Using CliMA-Land

We also used simulations from the Climate Model Alliance Land model (CliMA-Land) (Holtzman et al., 2023; Wang et al., 2021). CliMA-Land is a highly scalable model that incorporates key processes within the Soil-Plant-Atmosphere-Continuum (Wang et al., 2021). CliMA-Land allows for the customization of the plant hydraulic system. Vertically resolved plant hydraulics are incorporated into the model, with each organ characterized by its water potential and hydraulic conductivity. To capture the dynamic water storage within vegetation, CliMA-Land introduces a parameter linked to capacitance, representing a range of hydraulic strategies (Holtzman et al., 2023). In the context of simulating vegetation water content, the model enables a linear pressure-volume curve on leaf water potential to derive VOD in forms of VOD = $(1 + a^*\psi_{leaf})^*(b + c^*\text{LAI})$, where a, b, c are unknown parameters, which were retrieved using microwave brightness temperature from the AMSR-E and AMSR2 satellites as constraints. The model inputs include climate forcing of temperature, precipitation, relative humidity, downward short-wave radiation, long-wave radiation, and LAI. The model outputs include houly simulation of carbon fluxes, SMC, transpiration, and VOD, thus allowing for a direct comparison between the modeled VOD and the ground measurements of GNSS VOD on seasonal and diurnal time scales. The model simulation used here has been parameterized and optimized for the MOFLUX site. For more details, we refer the reader to Holtzman et al. (2023). The model simulation is used to investigate the mechanistic relationship between leaf water potential, plant transpiration and VOD.

2.3. Analysis

To disentangle environmental factors driving seasonal and diurnal VOD variations, we used Singular Value Decomposition (SVD) to decompose the VOD time series. We reshaped the VOD series as a matrix with days as the first dimension and hourly values as the second dimension, allowing us to discern the principal components in the diurnal cycles and their temporal loadings for each day. Subsequently, correlation analysis was used to identify the influencing factors on VOD seasonal and diurnal variations. Finally, the multiple linear regression analysis was used to estimate plant transpiration by linking VOD temporal loadings with plant transpiration. Specifically, modeled transpiration and eddy-covariance measured ET serve as the target variables in multiple linear regressions for model simulation and observation, respectively. It should be noted that VOD will only partially estimate the transpiration part of evapotranspiration.

3. Results

3.1. Decoding the Key Factors Affecting Seasonal Variations of GNSS VOD

VOD varied seasonally, reaching maxima during the peak growing season in June and July, after which it slowly declined until autumn leaf senescence. This can be explained by the greater leaf biomass and thus increased vertically integrated canopy water, resulting in higher VOD (Figure 1a). To understand factors impacting seasonal

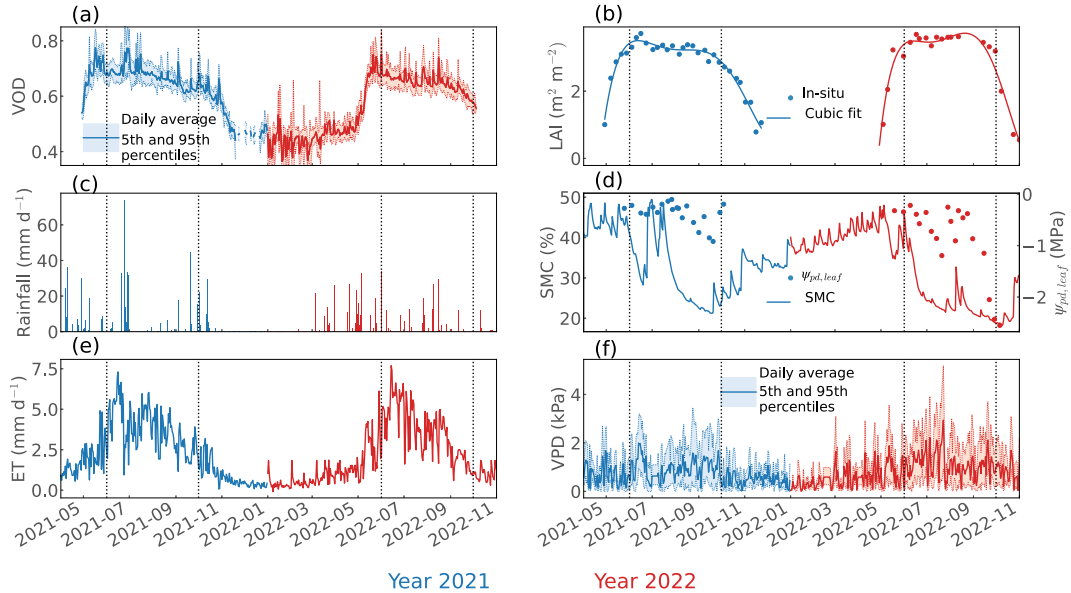

Figure 1. Time series of (a) daily averaged vegetation optical depth (VOD), (b) leaf area index (LAI), (c) rainfall events and (d) surface soil moisture content (SMC) shown as line and community predawn leaf water potential ($\psi_{pd,leaf}$) shown as dots, (e) evapotranspiration (ET) and (f) vapor pressure deficit (VPD) during the growing season in 2021 and 2022. In panel (b), a cubic fit on LAI records is applied to remove week-to-week variations. The blue and red lines denote the observations for 2021 and 2022, respectively. June 1st and Oct 1st are labeled in all panels for clarity.

VOD variations, we examined the relationship between VOD and other environmental factors. The rapid VOD increase during spring is associated with rapid leaf flushing, as evidenced in the observed LAI increase (Figure 1b). Moreover, VOD spikes during the growing season correspond well with the occurrence of rainfall events (Figure 1c), where a portion of the rainfall is intercepted by the plant canopy and subsequently re-evaporated. During the middle to late stages of summer (around July to August), the VOD decrease aligns with soil drying, as manifested by the drop in surface SMC despite short-term spikes induced by rainfall events (Figure 1d). The temporal variability of ET and VPD was compared here as well. On a seasonal scale, VOD is weakly correlated with ET ($R = 0.3$, Figure 1e) and VPD ($R = -0.28$, Figure 1f).

A quantitative partitioning of influences on VOD at daily time scales (when these factors exhibit less coupling) is illustrated in Figure S1 in Supporting Information S1. VOD loss was primarily influenced by surface soil drying, wherein the depletion of soil water diminished the plant's rehydration capacity. A decrease in LAI also notably contributed to a decline in VOD. Although diurnal temperature amplitude is recognized for its negative impact on latent heat flux, its influence on VOD reduction was not significant. A detailed method description can be found in Text S1 in Supporting Information S1.

During summer, we observed a decrease in in situ measurements of $\psi_{pd,leaf}$, which was mirrored by a decrease in VOD (Figures 1a and 1d). There is no uniform exact time of $\psi_{pd,leaf}$ sampling, which makes it hard to align the timing of VOD measurement with $\psi_{pd,leaf}$. We thus used the daily maximum VOD in the comparison with $\psi_{pd,leaf}$ as it usually appears in the pre-dawn. Figure 2a illustrates a clear positive relationship between the daily maximum VOD and $\psi_{pd,leaf}$ ($R^2 = 0.68$). In other words, lower VOD values coincide with a less hydrated canopy, as expected. This relationship is still significant when using VOD at 6 a.m. instead of daily maximum VOD, albeit with a lower correlation coefficient ($R^2 = 0.57$ in Figure S2 in Supporting Information S1). This strong relationship confirms the feasibility of using less labor-intensive measurement of GNSS VOD as a proxy for the monitoring of leaf water potential, like the relationship between radiometer-based VOD and leaf water potential in Holtzman et al. (2021). The daily anomaly relationship between VOD and $\psi_{pd,leaf}$ after subtracting their monthly average is also significant although it turns out to be weaker ($R^2 = 0.50$ in Figure S3 in Supporting Information S1). Subtracting the monthly average may assist in mitigating potential inflation in the covariance between VOD and $\psi_{pd,leaf}$, which stems from the influence of confounding seasonal periodicity. Importantly, our study represents the first validation of the relationship between GNSS VOD and leaf water potential.

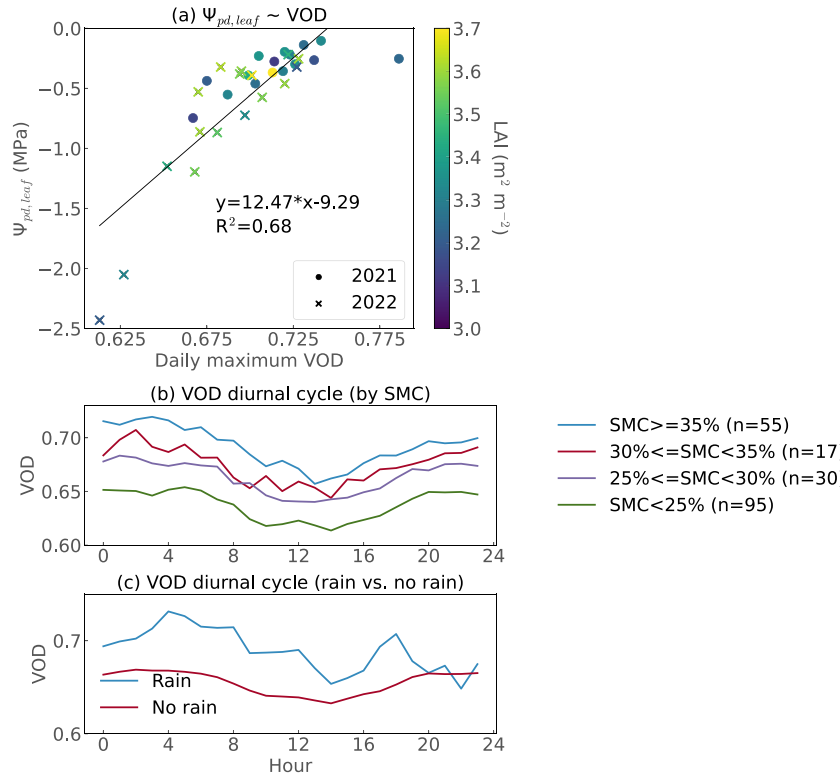

Figure 2. The (a) relationship between community predawn leaf water potential ($\psi_{pd,leaf}$) and daily maximum vegetation optical depth (VOD) for the year 2021 and 2022 and average diurnal cycle of VOD grouped by (b) varying water stress conditions denoted by SMC, (c) rainfall events. For example, the VOD in the "Rain" bins at 6 a.m. signifies the averaged VOD over all rainy instances at 6 a.m., while the VOD in the "No rain" bins at 6 a.m. represents the averaged VOD over non-rainy instances at 6 a.m. Only measurements made during the stable LAI period (LAI > 3.0 m^2 m^{-2}) and non-rainy period were used for panels (a, b).

3.2. Diurnal Variations of VOD

GNSS VOD yields continuous observations, providing a detailed picture of water dynamics at shorter time intervals. The diurnal VOD cycle reveals consistent patterns under varying moisture conditions (categorized by SMC), with higher values always observed in the morning and evening, and lower values around noon (Figure 2b). This pattern can be attributed to the typical peak in plant transpiration around noon, resulting in a decrease in plant water content and thus lower VOD. Before sunrise and after sunset, however, soil water replenishes the leaf water content. In addition to the impact of plant transpiration, at the diurnal scale, variations in leaf surface water lead to VOD changes as shown by the VOD comparison between "rain" and "no rain" categories at different times, thereby amplifying the VOD diurnal amplitude as well (Figure 2c). A more distinct diurnal pattern can be found when VOD was normalized by its daily maximum (Figure S4 in Supporting Information S1).

To identify the primary modes of diurnal variability of GNSS VOD, we further employed Singular Value Decomposition (SVD) on all diurnal cycles stacked over the non-rainy measurement period. This decomposition enabled us to extract the principal components (PC) and their temporal loadings (Figures 3a–3c). Given that the first three PCs collectively accounted for more than 99% of the total variance, our focus was on these three PCs and their associated temporal loadings. The 1st PC captures the mean diurnal cycle (Figure 3a, Figure S5 in Supporting Information S1), characterized by lower values around noon and higher values in the pre-dawn and nighttime. Moving on to the 2nd PC from GNSS VOD, it reflects a contrast between the morning and afternoon, that is, positive values in the early morning and negative values in the late afternoon. This contrast is likely attributable to a mixture of surface wetness from dew formation in the pre-dawn hours and subsequent re-evaporation throughout the day and leaf water potential drop. The 3rd PC, also centered around 0, modulates the diurnal amplitude of VOD but with an earlier peak time. We further examined the factors impacting the

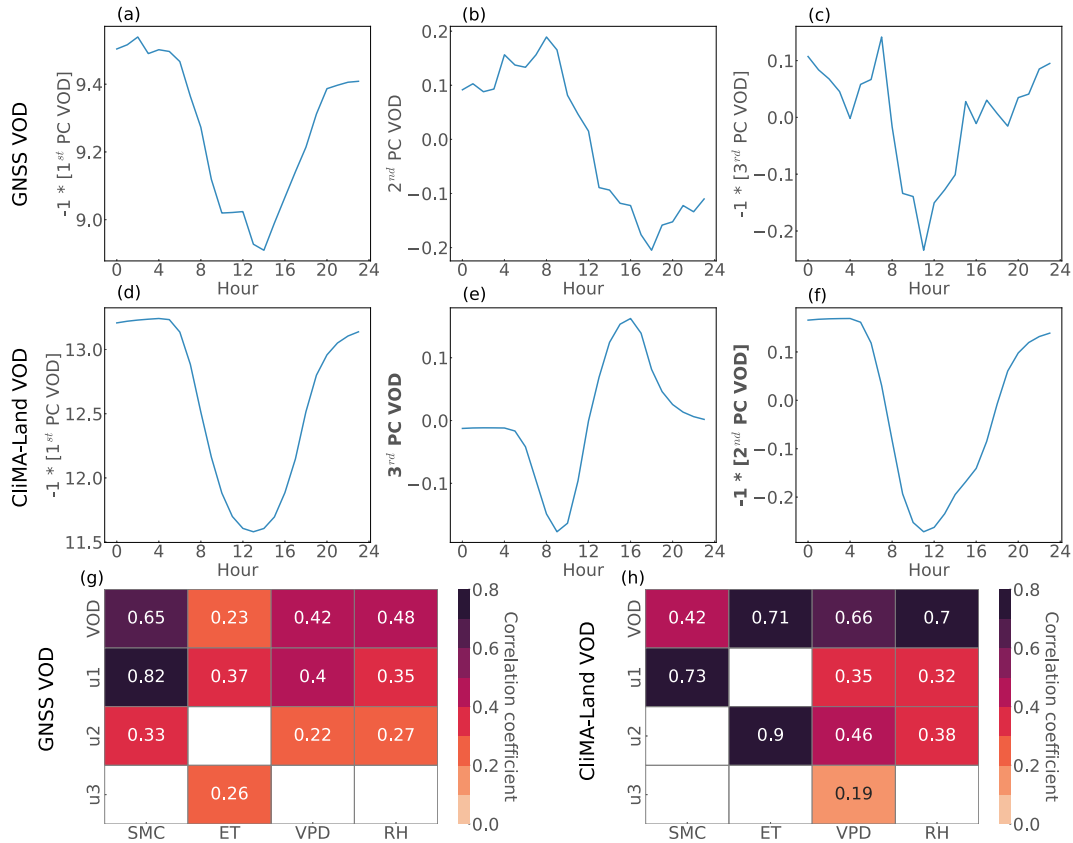

Figure 3. VOD time series decomposed by SVD. (a–c) GNSS VOD, (d–f) CliMA-Land VOD, (g, h) correlation matrix for time series of VOD and its principal components. Since the 2nd PC in CliMA-Land VOD resembles the 3rd PC in GNSS VOD, the order of the 2nd and 3rd PC in CliMA-Land VOD was swapped for clear comparison and their *y* axis labels were bold. In panel (g, h), the Pearson correlation coefficient was labeled only when there is a significant correlation ($P < 0.05$). In the matrices in (g, h), the "VOD" row shows correlation analysis for the total diurnal cycles. The rows "u1" to "u3" are for the correlation between the VOD temporal loadings and other variables across the season. Only measurements made during the stable LAI period (LAI > 3.0 m^2 m^{-2}) were used. A negative sign (−1) on the *y*-axis corresponds to a sign convention used to align with the typical diurnal pattern of VOD. The principal components shown here are scaled by their corresponding singular values.

temporal loadings of these PCs throughout the season using correlation analysis. The temporal loading of the 1st PC exhibited a correlation with SMC, suggesting that soil water plays a dominant role in driving the magnitude of plant water content during the growing season when LAI is not changing much, that is, higher SMC leads to higher VOD in a broad sense and subsequently a larger diurnal amplitude (Figure 3g). In the case of the 2nd PC, the spikes in its temporal loading correspond to relatively high levels of humidity and its correlation with daily maximum relative humidity is significant, which is a prerequisite for dew formation. The reconstruction of the VOD diurnal cycle from the 1st and 2nd PCs relative to the 1st PC only also shows a larger difference in the morning which gradually reduces (Figure S6 in Supporting Information S1). The earlier peak in the 3rd PC is influenced by the peak time of daily ET, as daily ET usually reaches its peak around 12 p.m. (Figure S7 in Supporting Information S1). The temporal loading of the 3rd PC correlates with daily ET (Figure 3g), indicating that increased ET leads to a larger VOD diurnal amplitude due to greater consumption of plant water for transpiration.

The CliMA-Land model simulates VOD based on LAI and leaf water potential, with calibration against brightness temperature observations. Since stomatal conductance relies on leaf water potential and transpiration is influenced by LAI and stomatal conductance together, the variation in VOD diurnal amplitude in the CliMA-Land model is inherently linked to plant transpiration. As a result, the CliMA-Land simulation aids in interpreting the VOD diurnal amplitude. The CliMA-Land model's VOD simulation closely aligns with GNSS VOD, exhibiting similar seasonality and diurnal patterns (see Figures S8–S10 in Supporting Information S1). This alignment

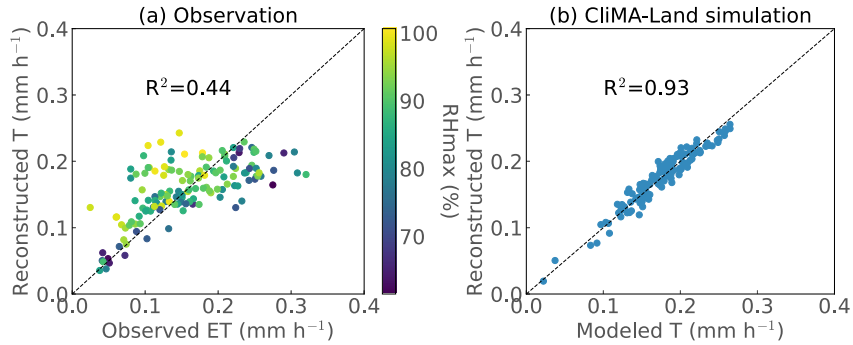

Figure 4. Plant transpiration reconstructed by VOD PCs during soil drydown periods with SMC < 35% when VOD is unaffected by rainfall pulses. (a) GNSS VOD, (b) CliMA-Land VOD. Only measurements made during the stable LAI period (LAI > 3.0 m^2 m^{-2}) were used.

enables the validation of the GNSS VOD decomposition interpretation. We performed a similar decomposition on the VOD time series generated by the CliMA-Land model (Figures 3d–3f). Remarkably, the shapes of the 1st and 2nd PC in the CliMA-Land VOD strongly resemble those of the 1st and 3rd PC identified in the GNSS VOD analysis, albeit with a smoother profile for the latter. The 1st PC still represents a mean diurnal cycle (Figure S11 in Supporting Information S1), and the 2nd PC exhibits a unimodal shape as well. In line with the observations, the temporal loading of the 1st PC in the CliMA-Land VOD correlates with surface SMC (Figure 3h). Moreover, the time series of the 2nd PC is significantly correlated with daily ET (Figure 3h), reaffirming the modulation of ET on the VOD diurnal amplitude.

The similarities between the principal components of the GNSS VOD and CliMA-Land simulated VOD provide evidence to support our interpretation of the biophysical causes of the PC and their loadings. While the CliMA-Land simulations are also uncertain, their similarity to the GNSS VOD provides confidence that the diurnal and seasonal patterns analyzed above are accurately represented in CliMA-Land. We therefore further hypothesize that the majority of the differences between GNSS VOD and CliMA-Land VOD are primarily linked to leaf surface water including intercepted water and dew (which are not represented in CliMA-Land but possibly influence the GNSS VOD, Figure 2c), rather than plant hydraulics per se.

3.3. ET Reconstruction

It is worth noting that the major component of ET in forested environments, plant transpiration, is linked to the leaf-soil water potential gradient, which governs the vertical water supply. Through multiple linear regression, we found a notable correlation between the principal components of GNSS VOD and observed ET, and between modeled VOD and modeled transpiration in the CliMA-Land model. In other words, both CliMA-Land model and observation agree that transpiration can be predicted from VOD components, although the correlation coefficient is relatively lower in observations compared to the model simulation (R^2 = 0.44 vs. R^2 = 0.93 in Figure 4). While originating from a similar regression format, these two models were trained separately, resulting in distinct coefficients. It should be noted that such reconstruction tends to underestimate ET when observed ET is high, possibly because VOD can only account for plant transpiration and cannot capture soil evaporation dynamics.

Physiologically, it makes sense that both mean VOD (1st PC) and the strength of the diurnal VOD amplitude (3rd PC) are somewhat related to ET. First, VOD is closely tied to vegetation water content, which in turn is related to leaf water potential. The temporal loading of the 1st PC reflects changes in overall VOD magnitude (Figure S12 in Supporting Information S1), and therefore in leaf water potential. As transpiration is largely controlled by the water potential gradient, the temporal loading of the 1st PC should be related in some way to transpiration. Second, the 3rd PC of GNSS VOD reflects shifts in the diurnal amplitude of VOD. Producing a large diurnal amplitude likely implies a large transpiration flux, one that would be sufficiently strong to severely deplete canopy water content during midday. Thus, it makes sense that the temporal loading of the 3rd PC also plays a role in determining the magnitude of daily ET. In summary, the temporal loadings of both the 1st and 3rd PC contribute to the overall ET magnitude.

4. Discussion and Conclusion

In this study, we investigated the seasonal and diurnal variations in VOD obtained from the GNSS technique. VOD dynamics indicate both changes in biomass and relative water content within vegetation. While biomass and water content exhibit temporal and spatial covariation, water content dynamics can be discerned at finer time scales, whereas biomass gain or loss occurs over longer periods. The GNSS technique offers a promising opportunity to track the diurnal VOD cycle. Here, it enables our exploration of physiological processes such as plant transpiration and water potential dynamics with few confounding effects from changes in canopy structure.

We found a strong correlation between GNSS VOD and $\psi_{pd,leaf}$. Previous studies have examined similar relationships using passive VOD measurements at both X-band (Momen et al., 2017; Zhang et al., 2019) and L-band (Holtzman et al. (2021). However, Momen et al. (2017) and Zhang et al. (2019) were subject to large scaling errors as they compared only a few points with relatively large spaceborne pixels (e.g., 25 km). While the records used in Holtzman et al. (2021) cover a much shorter period (less than 1 week) compared to the GNSS VOD data set, the correlation coefficient is similar ($R = 0.76$ in Holtzman et al. (2021) vs. $R = 0.83$ in this work). The robust correlation measured here across two summers underscores the potential of the GNSS technique for VOD observations, offering a practical proxy to labor-intensive measurements of leaf water potential.

In addition to its potential to complement leaf water potential measurements, our investigation into the VOD diurnal cycle has unveiled the modulating effects of leaf surface water and plant transpiration on the shift of VOD diurnal amplitude. GNSS VOD reflects the total canopy water, allowing for inference of leaf surface water dynamics as well. The impact of canopy surface water on VOD can vary significantly depending on the canopy structure and meteorological conditions (Holtzman et al., 2021; Khabbazan et al., 2022; Xu et al., 2021). The morning-afternoon contrast shown in the 2nd PC of GNSS VOD likely arises from dew formation in the pre-dawn followed by re-evaporation over the course of the day (Figure S6 in Supporting Information S1). Separating the contributions of leaf surface water from plant internal water content, will help further understanding of water movements within vegetation canopies.

Furthermore, VOD reflects the amount of vegetation water content, which behaves as a buffer against xylem tension induced by plant transpiration (Köcher et al., 2013). Increased transpiration leads to greater depletion of leaf water storage, resulting in a larger VOD diurnal amplitude. Since the transpiration water supply can be approximated as the product of hydraulic conductivity and the water potential gradient, both of which are influenced by leaf water potential, the temporal loadings of VOD PCs correlate with plant transpiration during the soil drydown periods (i.e., when VOD is unaffected by rainfall pulses), suggesting that such VOD measurement is a new possible method for estimating plant transpiration. Several ET partitioning methods have been proposed in the literature (Li et al., 2019; Nelson et al., 2018; Zhou et al., 2016), though they remain uncertain. Considering the impact of plant transpiration and leaf surface water on diurnal amplitude of VOD, our GNSS VOD data offer an alternative perspective for efforts related to ET partitioning. The regression formula used for reconstruction can capture the influences of factors such as water potential and changes in water storage. The varying coefficients for the PCs in the formula indicate the relative significance of these driving factors on the magnitude of plant transpiration. These coefficients can also fluctuate among different water use strategies (Bartlett et al., 2019). This approach serves as an initial endeavor in developing a new ET partitioning method, though its reliability should be further investigated through sap flux measurements across a range of sites. Such observationally derived plant transpiration data holds great promise as valuable constraints for enhancing model simulations (Cui et al., 2023).

Our work carries several important implications. The use of continuous GNSS-based VOD monitoring emerges as an effective strategy for addressing the information gap pertaining to water potential (Novick et al., 2022). We have demonstrated a strong correlation between VOD and leaf water potential, validated against in situ field measurements. As geostationary microwave satellites are currently not available, we recommend more deployments of these promising, lower-cost yet robust instruments at existing flux tower sites. This will provide complementary measurements to assess carbon and water fluxes, effectively bridging the gap in our understanding of vegetation water content and its temporal dynamics. We highlighted that such VOD observations are at the same temporal resolutions as flux measurements and align well with the flux footprint compared to conventional automated measurements of water status.

Data Availability Statement

Ecosystem flux data for US-MOz is available at Wood and Gu (2022). Predawn leaf water potential measurement is available at Pallardy et al. (2018). CliMA-Land model is open-sourced, and is available at N. Holtzman (2023).

Acknowledgments
This work was supported by NASA Carbon Cycle Science Grant 80NSSC21K1712. AGK was also supported by the Alfred P.Sloan Foundation.

References

Anderegg, W. R., Konings, A. G., Trugman, A. T., Yu, K., Bowling, D. R., Gabbitas, R., et al. (2018). Hydraulic diversity of forests regulates ecosystem resilience during drought. *Nature*, *561*(7724), 538–541. https://doi.org/10.1038/s41586-018-0539-7

Barraclough, A. D., Cusens, J., Zweifel, R., & Leuzinger, S. (2020). Environmental drivers of stem radius change and heterogeneity of stem radial water storage in the mangrove Avicennia marina (Forssk.) Vierh. *Agricultural and Forest Meteorology*, *280*, 107764. https://doi.org/10.1016/j.agrformet.2019.107764

Bartlett, M. K., Detto, M., & Pacala, S. W. (2019). Predicting shifts in the functional composition of tropical forests under increased drought and CO_2 from trade-offs among plant hydraulic traits. *Ecology Letters*, *22*(1), 67–77. https://doi.org/10.1111/ele.13168

Bueso, D., Piles, M., Ciais, P., Wigneron, J.-P., Moreno-Martínez, Á., & Camps-Valls, G. (2023). Soil and vegetation water content identify the main terrestrial ecosystem changes. *National Science Review*, *10*(5), nwad026. https://doi.org/10.1093/nsr/nwad026

Cui, J., He, M., Lian, X., Wei, Z., & Wang, T. (2023). Spatial pattern of plant transpiration over China constrained by observations. *Geophysical Research Letters*, *50*(20), e2023GL105489. https://doi.org/10.1029/2023GL105489

Fan, L., Wigneron, J.-P., Ciais, P., Chave, J., Brandt, M., Fensholt, R., et al. (2019). Satellite-observed pantropical carbon dynamics. *Nature Plants*, *5*(9), 944–951. https://doi.org/10.1038/s41477-019-0478-9

Gentine, P., Green, J. K., Guérin, M., Humphrey, V., Seneviratne, S. I., Zhang, Y., & Zhou, S. (2019). Coupling between the terrestrial carbon and water cycles—A review. *Environmental Research Letters*, *14*(8), 083003. https://doi.org/10.1088/1748-9326/ab22d6

Gu, L., Pallardy, S. G., Hosman, K. P., & Sun, Y. (2015). Drought-influenced mortality of tree species with different predawn leaf water dynamics in a decade-long study of a central US forest. *Biogeosciences*, *12*(10), 2831–2845. https://doi.org/10.5194/bg-12-2831-2015

Gu, L., Pallardy, S. G., Hosman, K. P., & Sun, Y. (2016). Impacts of precipitation variability on plant species and community water stress in a temperate deciduous forest in the central US. *Agricultural and Forest Meteorology*, *217*, 120–136. https://doi.org/10.1016/j.agrformet.2015.11.014

Gu, L., Pallardy, S. G., Yang, B., Hosman, K. P., Mao, J., Ricciuto, D., et al. (2016). Testing a land model in ecosystem functional space via a comparison of observed and modeled ecosystem flux responses to precipitation regimes and associated stresses in a Central US forest. *Journal of Geophysical Research: Biogeosciences*, *121*(7), 1884–1902. https://doi.org/10.1002/2015jg003302

Harris, B. L., Taylor, C. M., Weedon, G. P., Talib, J., Dorigo, W., & Van Der Schalie, R. (2022). Satellite-observed vegetation responses to intraseasonal precipitation variability. *Geophysical Research Letters*, *49*(15), e2022GL099635. https://doi.org/10.1029/2022gl099635

He, H., Turner, N. C., Aogu, K., Dyck, M., Feng, H., Si, B., et al. (2021). Time and frequency domain reflectometry for the measurement of tree stem water content: A review, evaluation, and future perspectives. *Agricultural and Forest Meteorology*, *306*, 108442. https://doi.org/10.1016/j.agrformet.2021.108442

Holtzman, N. (2023). CliMa_Microwave [Software]. *GITHUB*. https://github.com/natan-holtzman/CliMa_Microwave

Holtzman, N., Wang, Y., Wood, J. D., Frankenberg, C., & Konings, A. G. (2023). Constraining plant hydraulics with microwave radiometry in a land surface model: Impacts of temporal resolution. *Water Resources Research*, *59*(11), e2023WR035481. https://doi.org/10.1029/2023wr035481

Holtzman, N. M., Anderegg, L. D., Kraatz, S., Mavrovic, A., Sonnentag, O., Pappas, C., et al. (2021). L-band vegetation optical depth as an indicator of plant water potential in a temperate deciduous forest stand. *Biogeosciences*, *18*(2), 739–753. https://doi.org/10.5194/bg-18-739-2021

Humphrey, V., & Frankenberg, C. (2023). Continuous ground monitoring of vegetation optical depth and water content with GPS signals. *Biogeosciences*, *20*(9), 1789–1811. https://doi.org/10.5194/bg-20-1789-2023

Jagdhuber, T., Fluhrer, A., Schmidt, A.-S., Jonard, F., Chaparro, D., Meyer, T., et al. (2021). Retrieval of forest water potential from L-band vegetation optical depth. In *2021 IEEE international geoscience and remote sensing symposium IGARSS*.

Khabbazan, S., Steele-Dunne, S., Vermunt, P., Judge, J., Vreugdenhil, M., & Gao, G. (2022). The influence of surface canopy water on the relationship between L-band backscatter and biophysical variables in agricultural monitoring. *Remote Sensing of Environment*, *268*, 112789. https://doi.org/10.1016/j.rse.2021.112789

Köcher, P., Horna, V., & Leuschner, C. (2013). Stem water storage in five coexisting temperate broad-leaved tree species: Significance, temporal dynamics and dependence on tree functional traits. *Tree Physiology*, *33*(8), 817–832. https://doi.org/10.1093/treephys/tpt055

Konings, A. G., Rao, K., & Steele-Dunne, S. C. (2019). Macro to micro: Microwave remote sensing of plant water content for physiology and ecology. *New Phytologist*, *223*(3), 1166–1172. https://doi.org/10.1111/nph.15808

Konings, A. G., Saatchi, S. S., Frankenberg, C., Keller, M., Leshyk, V., Anderegg, W. R., et al. (2021). Detecting forest response to droughts with global observations of vegetation water content. *Global Change Biology*, *27*(23), 6005–6024. https://doi.org/10.1111/gcb.15872

Li, X., Gentine, P., Lin, C., Zhou, S., Sun, Z., Zheng, Y., et al. (2019). A simple and objective method to partition evapotranspiration into transpiration and evaporation at eddy-covariance sites. *Agricultural and Forest Meteorology*, *265*, 171–182. https://doi.org/10.1016/j.agrformet.2018.11.017

Matheny, A. M., Bohrer, G., Garrity, S. R., Morin, T. H., Howard, C. J., & Vogel, C. S. (2015). Observations of stem water storage in trees of opposing hydraulic strategies. *Ecosphere*, *6*(9), 1–13. https://doi.org/10.1890/es15-00170.1

McDowell, N. G., Sapes, G., Pivovaroff, A., Adams, H. D., Allen, C. D., Anderegg, W. R., et al. (2022). Mechanisms of woody-plant mortality under rising drought, CO_2 and vapour pressure deficit. *Nature Reviews Earth & Environment*, *3*(5), 294–308. https://doi.org/10.1038/s43017-022-00272-1

Momen, M., Wood, J. D., Novick, K. A., Pangle, R., Pockman, W. T., McDowell, N. G., & Konings, A. G. (2017). Interacting effects of leaf water potential and biomass on vegetation optical depth. *Journal of Geophysical Research: Biogeosciences*, *122*(11), 3031–3046. https://doi.org/10.1002/2017jg004145

Nelson, J. A., Carvalhais, N., Cuntz, M., Delpierre, N., Knauer, J., Ogée, J., et al. (2018). Coupling water and carbon fluxes to constrain estimates of transpiration: The TEA algorithm. *Journal of Geophysical Research: Biogeosciences*, *123*(12), 3617–3632. https://doi.org/10.1029/2018jg004727

Novick, K. A., Ficklin, D. L., Baldocchi, D., Davis, K. J., Ghezzehei, T. A., Konings, A. G., et al. (2022). Confronting the water potential information gap. *Nature Geoscience*, *15*(3), 158–164. https://doi.org/10.1038/s41561-022-00909-2

Pallardy, S. G., Gu, L., Wood, J. D., Hosman, K. P., & Sun, Y. (2018). Predawn leaf water potential of oak-hickory forest at Missouri Ozark (MOFLUX) site: 2004–2021 [Dataset]. *Oak Ridge National Laboratory, TES SFA, U.S. Department of Energy*. https://doi.org/10.3334/CDIAC/ornlsfa.004

Rodriguez-Alvarez, N., Bosch-Lluis, X., Camps, A., Ramos-Perez, I., Valencia, E., Park, H., & Vall-Llossera, M. (2011). Vegetation water content estimation using GNSS measurements. *IEEE Geoscience and Remote Sensing Letters*, *9*(2), 282–286. https://doi.org/10.1109/lgrs.2011.2166242

Smith, T., Traxl, D., & Boers, N. (2022). Empirical evidence for recent global shifts in vegetation resilience. *Nature Climate Change*, *12*(5), 477–484. https://doi.org/10.1038/s41558-022-01352-2

Wang, Y., Köhler, P., He, L., Doughty, R., Braghiere, R. K., Wood, J. D., & Frankenberg, C. (2021). Testing stomatal models at the stand level in deciduous angiosperm and evergreen gymnosperm forests using CliMA Land (v0. 1). *Geoscientific Model Development*, *14*(11), 6741–6763. https://doi.org/10.5194/gmd-14-6741-2021

Wood, J., & Gu, L. (2022). AmeriFlux FLUXNET-1F US-MOz Missouri Ozark site [Dataset]. *AMF*. https://doi.org/10.17190/AMF/1854370

Wood, J. D., Gu, L., Hanson, P. J., Frankenberg, C., & Sack, L. (2023). The ecosystem wilting point defines drought response and recovery of a Quercus-Carya forest. *Global Change Biology*, *29*(7), 2015–2029. https://doi.org/10.1111/gcb.16582

Wood, J. D., Widmer, B. W., Anderson, D., Pallardy, S. G., Gu, L., & Hosman, K. P. (2022). Leaf-area index of oak-hickory forest at Missouri Ozark (MOFLUX) site: 2007–2022 [Dataset]. *OSTI.GOV*. https://doi.org/10.25581/ornlsfa.028/1906782

Xu, X., Konings, A. G., Longo, M., Feldman, A., Xu, L., Saatchi, S., et al. (2021). Leaf surface water, not plant water stress, drives diurnal variation in tropical forest canopy water content. *New Phytologist*, *231*(1), 122–136. https://doi.org/10.1111/nph.17254

Yang, H., Ciais, P., Wigneron, J.-P., Chave, J., Cartus, O., Chen, X., et al. (2022). Climatic and biotic factors influencing regional declines and recovery of tropical forest biomass from the 2015/16 El Niño. *Proceedings of the National Academy of Sciences*, *119*(26), e2101388119. https://doi.org/10.1073/pnas.2101388119

Zhang, R., Kim, S., Sharma, A., & Lakshmi, V. (2021). Identifying relative strengths of SMAP, SMOS-IC, and ASCAT to capture temporal variability. *Remote Sensing of Environment*, *252*, 112126. https://doi.org/10.1016/j.rse.2020.112126

Zhang, Y., Zhou, S., Gentine, P., & Xiao, X. (2019). Can vegetation optical depth reflect changes in leaf water potential during soil moisture dry-down events? *Remote Sensing of Environment*, *234*, 111451. https://doi.org/10.1016/j.rse.2019.111451

Zhou, S., Yu, B., Zhang, Y., Huang, Y., & Wang, G. (2016). Partitioning evapotranspiration based on the concept of underlying water use efficiency. *Water Resources Research*, *52*(2), 1160–1175. https://doi.org/10.1002/2015wr017766

References From the Supporting Information

Feldman, A. F., Short Gianotti, D. J., Trigo, I. F., Salvucci, G. D., & Entekhabi, D. (2020). Land-atmosphere drivers of landscape-scale plant water content loss. *Geophysical Research Letters*, *47*(22), e2020GL090331. https://doi.org/10.1029/2020gl090331

Feldman, A. F., Short Gianotti, D. J., Trigo, I. F., Salvucci, G. D., & Entekhabi, D. (2022). Observed landscape responsiveness to climate forcing. *Water Resources Research*, *58*(1), e2021WR030316. https://doi.org/10.1029/2021wr030316

Panwar, A., Kleidon, A., & Renner, M. (2019). Do surface and air temperatures contain similar imprints of evaporative conditions? *Geophysical Research Letters*, *46*(7), 3802–3809. https://doi.org/10.1029/2019gl082248